JOURNAL OF MATERIALS SCIENCE 9 (1974) 100–108

Elastic and thermal expansion anisotropy of oriented linear polyethylene

C. P. BUCKLEY
Department of Engineering Science, Oxford University, Oxford, UK

A two-phase composite laminate model is proposed for representing biaxially oriented sheets of linear polyethylene. Thermoelastic analysis of the model yields predictions of the complete elastic and thermal expansion anisotropy. These predictions are compared with experimental measurements of elastic compliance and thermal expansivity obtained with the same oriented sheets. Using only one adjustable parameter (Poisson's ratio of non-crystalline linear polyethylene), extensive qualitative agreement is obtained between model predictions and experimental results. Discrepancies which are observed are attributed to the influence of the interfacial regions which exist between adjacent stacks of lamellar crystals in the real oriented sheets.

1. Introduction

When linear polyethylene (LPE) is oriented by drawing and then annealing at temperatures between 120 and 130°C, the resulting microstructure has a lamellar texture. Electron microscopy [1-3] and small-angle X-ray scattering [4-6] show the structure to consist of stacks of lamellar crystals, of thickness *c.* 300 Å, separated by layers of non-crystalline polymer, of thickness *c.* 50 Å. A characteristic lamellar texture also dominates the morphology of undrawn melt-crystallized LPE and the majority of other polymers of high crystallinity [7]. Such a texture strikingly resembles the lay-up of the phases in a two-phase composite laminated solid which, therefore, may be a useful analogue for the purpose of understanding, for example, thermoelastic behaviour of these polymers.

Several authors have, in essence, proposed a composite laminate model for predicting the elastic properties of semicrystalline polymers of medium or high crystallinity. Maeda *et al* [8] suggested implicitly (model I of their paper) that the structural unit in such polymers be taken to consist of a two-phase composite laminate arrangement of crystalline and non-crystalline regions and calculated its compliance matrix. Halpin and Kardos [9] described a method for predicting the macroscopic elastic moduli of such polymers, representing the polymer by an amorphous matrix containing lamellar crystalline inclusions. Owen and Ward [10] represented sheets of oriented branched polyethylene by a model of alternating ribbon-like layers of crystalline and non-crystalline polymer, for the purpose of predicting elastic anisotropy.

The present work explores the ability of a composite laminate model to correctly predict elastic and thermal expansion anisotropy of oriented LPE. Advantage is taken of drawn and annealed sheets of LPE in which crystal *a*-, *b*- and *c*-axes and lamella normals n_1 have simple singlet or doublet preferred orientations. Each oriented sheet is modelled by a three-dimensional composite laminate solid. Simple thermoelastic analysis then predicts the complete anisotropy of both elastic compliance and thermal expansivity. The success of the model is judged by comparing these predictions with experimental results obtained with the real oriented sheet.

This paper forms a sequel to previous work [11-13] in which mechanical coupling between crystalline and non-crystalline regions in oriented LPE was represented by simple linear models of the type proposed by Takayanagi *et al* [14]. The equations of the simple series and parallel models used before, are first approximations to those derived from the present model [15]. The complete composite laminate treatment, however, can decide which of the previously noted discrepancies between theory and experiment [13] arise from the neglect, inherent in the assumption of linear coupling, of the predominantly lamellar microstructure.

2. Experimental

The oriented sheets of LPE studied here have been described in detail elsewhere [16]. They were prepared by drawing, at constant width, compression moulded plates of Rigidex 2 (BP Chemicals Ltd) which were subsequently annealed for 1 h at 127°C. Crystallographic and lamella orientation with respect to axes, X, Y, Z, defined as in Fig. 1, were determined by wide-angle and small-angle X-ray diffraction respectively. Drawing x7 at room temperature gave double preferred orientation with a-axes in the ZX plane at $\pm 5°$ to X, b axes parallel to Y, c-axes in the ZX plane at $\pm$ 5° to Z and n_1 in the ZX plane at $\pm$ 38° to Z. Drawing x9 in air at 120°C, however, gave the single scheme of preferred orientation with a-axes parallel to X, b-axes parallel to Y and c-axes and n_1 parallel to Z. These two types of drawn sheet will here be designated "biaxially cold-drawn" LPE and "biaxially hot-drawn" LPE, respectively. They had crystal volume fractions χ_v of 0.81 [12] and 0.80 [13], respectively, as estimated from density (and, in the former case, gas solubility) measurements.

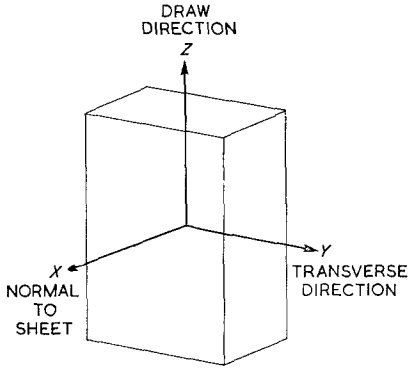

Figure 1 Definition of directions X, Y, Z in a drawn sheet of LPE.

From the oriented sheets rectangular specimens (0.1 cm × 0.3 cm × 3.5 cm) were cut with their long axes in the YZ plane at various angles $\theta°$ to Z. For each specimen the tensile creep compliance $D_\theta{}^T(t)$ was measured over the range of temperature T from −190 to −60°C using the procedure outlined previously [16]. Tensile strains were always less than 0.001 and all specimens always deformed as linear viscoelastic solids to within the sensitivity of measurement. Results will be presented here as isochronal values for a creep time, t, of 10 sec.

Identical rectangular specimens were used for measuring linear thermal expansivity e in the YZ plane (e is defined as $(l_T - l_0)l_0$ in terms of the specimen length l_T at T°C and l_0 at 0°C). Results were expressed as the linear thermal expansivities e_y and e_z measured parallel to Y and Z respectively. Measurements covered the temperature range −190 to 0°C and were obtained following the method described previously [13]. Linear thermal expansivity e_x parallel to X was obtained from e_y, e_z and the volumetric thermal expansivity e_v through the relation

$$1 + e_v = (1 + e_x)(1 + e_y)(1 + e_z) . \quad (1)$$

The method of Sauer *et al* [17], based on Archimedes' Principle, was used for determining e_v, a portion of the oriented sheet being suspended in a bath of ethanol while the temperature steadily rose from *c.* −120 to 0°C over a period of *c.* 40 h.

Of these measurements $D_0{}^T$ (10 sec) and $D_{90}{}^T$ (10 sec) for biaxially cold-drawn LPE [12] and e_x, e_y and e_z for biaxially hot-drawn LPE [13] have already been presented. In this paper, the complete set of results $D_0{}^T$ (10 sec), $D_{45}{}^T$ (10 sec) $D_{90}{}^T$ (10 sec), e_x, e_y and e_z for both biaxially cold-drawn and biaxially hot-drawn LPE will be used for assessing the composite laminate model.

3. Composite laminate model

3.1. Description

The model for representing a sheet of biaxially oriented LPE is shown in Fig. 2. It consists of two parallel stacks of parallel alternating lamellar layers of crystalline (C) and non-crystalline, or "amorphous" (A), LPE. Each stack occupies half the sheet thickness: they are perfectly bonded in the YZ plane, in which they are mirror-images. The volume fractions of phases A and C are respectively $1 - \chi_v$ and χ_v, measured for the real oriented sheet. The C/A/C repeat distance parallel to Z takes its mean value in the real sheet, while in width the layers of a given stack extend across its entire breadth and thickness. The orientations of lamella normals and crystal axes within one of the stacks are indicated in Fig. 2. Lamella normals n_1 lie in the ZX plane at an angle Ω to Z, crystal a- and c-axes also lie in the ZX plane, but at angles $(90° - \alpha)$ and $-\alpha$ to Z respectively, while

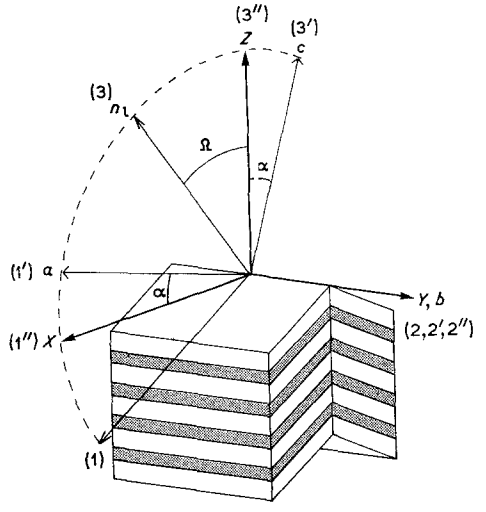

Figure 2 Schematic diagram of the two-phase composite laminate model for a sheet of biaxially oriented LPE: Phase A is shown grey, phase C white. Crystallographic and lamella orientations are indicated for the nearer stack of lamellae: those of the other stack are mirror-images in the *YZ* plane.

b-axes lie parallel to *Y*. Corresponding orientations in the other stack are simply mirror-images in the *YZ* plane. The angles Ω and α take their mean values in the real oriented sheet as measured by X-ray diffraction. A sheet of biaxially cold-drawn LPE is, therefore, represented by a model in which $\Omega = 38°$, $\alpha = 5°$, and a sheet of biaxially hot-drawn LPE by a model in which $\Omega = 0°$, $\alpha = 0°$.

In the analysis which follows, the two stacks are assumed to deform independently under the action of an applied stress or temperature change. For such a model this is true to a high degree of accuracy if the resulting overall strain in all directions in the plane of the interface is equal in the two stacks. Since occasions can arise when this condition is not fulfilled, a minor restriction must be placed on the application of the model described above (see Section 4.1).

3.2. Analysis

Consider the deformation of the model shown in Fig. 2 under the action of an applied stress system or change in temperature. The two stacks are assumed to deform independently (see above) and we therefore treat the deformation of a single stack alone. Within the stack define an orthogonal set of axes 1, 2, 3 with 2 parallel to *Y* and 3 parallel to n_1 as shown in Fig. 2. Assume both phases A and C to be homogeneous, anisotropic linear elastic continua with orthotropic symmetry, each phase having one axis of symmetry parallel to axis 2.

For convenience, we represent the second rank tensors of stress σ_{ij}, strain ϵ_{ij} and thermal expansivity e_{ij} by their corresponding 6-element column matrices $\boldsymbol{\sigma}$, $\boldsymbol{\epsilon}$ and $\mathbf{e}$ respectively, using the usual [18] contracted notation with the engineering definition of strain for both $\boldsymbol{\epsilon}$ and $\mathbf{e}$. Similarly we represent the fourth rank tensors of compliance S_{ijkl} and stiffness C_{ijkl} by their corresponding 6×6 matrices $\mathbf{S}$ and $\mathbf{C}$, derived from the same contracted notation. As written above they refer to the entire stack. When referring to phase A or C these symbols, and their matrix elements, carry the additional subscript a or c respectively.

The overall deformation of the stack in response to an applied stress system $\boldsymbol{\sigma}$ and temperature rise $\triangle T$ is given by the matrix equation

$$\boldsymbol{\epsilon} = \mathbf{S}\boldsymbol{\sigma} + \mathbf{e}(\triangle T) . \tag{2}$$

Similarly, the corresponding thermoelastic relations apply at every point in phase A

$$\boldsymbol{\epsilon}_a = \mathbf{S}_a\boldsymbol{\sigma}_a + \mathbf{e}_a(\triangle T) \tag{3}$$

and in phase C

$$\boldsymbol{\epsilon}_c = \mathbf{S}_c\boldsymbol{\sigma}_c + \mathbf{e}_c(\triangle T) . \tag{4}$$

As referred to axes 1, 2, 3, $\mathbf{e}$ and $\mathbf{S}$ have the forms

$$\mathbf{e} = \begin{bmatrix} e_1 \\ e_2 \\ e_3 \\ 0 \\ e_5 \\ 0 \end{bmatrix} \text{ and } \mathbf{S} = \begin{bmatrix} S_{11} & S_{12} & S_{13} & 0 & S_{15} & 0 \\ S_{12} & S_{22} & S_{23} & 0 & S_{25} & 0 \\ S_{13} & S_{23} & S_{33} & 0 & S_{35} & 0 \\ 0 & 0 & 0 & S_{44} & 0 & S_{46} \\ S_{15} & S_{25} & S_{35} & 0 & S_{55} & 0 \\ 0 & 0 & 0 & S_{46} & 0 & S_{66} \end{bmatrix}$$

while $\mathbf{e}_a$ and $\mathbf{e}_c$ take the same form as $\mathbf{e}$ and $\mathbf{S}_a$ and $\mathbf{S}_c$ the same form as $\mathbf{S}$.

For such a two-phase laminated solid to be in static equilibrium, the terms of $\boldsymbol{\sigma}_a$ and $\boldsymbol{\sigma}_c$ must [15] be related to those of $\boldsymbol{\sigma}$ through

$$\begin{aligned} \sigma_1 &= v_a\bar{\sigma}_{a1} + v_c\bar{\sigma}_{c1} \\ \sigma_2 &= v_a\bar{\sigma}_{a2} + v_c\bar{\sigma}_{c2} \\ \sigma_3 &= \bar{\sigma}_{a3} \quad\; = \bar{\sigma}_{c3} \\ \sigma_4 &= \bar{\sigma}_{a4} \quad\; = \bar{\sigma}_{c4} \\ \sigma_5 &= \bar{\sigma}_{a5} \quad\; = \bar{\sigma}_{c5} \\ \sigma_6 &= v_a\bar{\sigma}_{a6} + v_c\bar{\sigma}_{c6} \end{aligned} \tag{5}$$

where v_a and v_c denote the volume fractions $1 - \chi_v$ and χ_v of phases A and C respectively and a bar placed above denotes the volume average value. Similarly, if phases A and C are perfectly bonded, the condition of compatibility of displacement in each phase which must be

obeyed at all points in the interfaces between A and C requires [15] that ϵ be related to ϵ_a and ϵ_c through

$$\begin{aligned}
\epsilon_1 &= \bar{\epsilon}_{a1} &&= \bar{\epsilon}_{c1} \\
\epsilon_2 &= \bar{\epsilon}_{a2} &&= \bar{\epsilon}_{c2} \\
\epsilon_3 &= v_a\,\bar{\epsilon}_{a3} &&+ v_c\,\bar{\epsilon}_{c3} \\
\epsilon_4 &= v_a\,\bar{\epsilon}_{a4} &&+ v_c\,\bar{\epsilon}_{c4} \\
\epsilon_5 &= v_a\,\bar{\epsilon}_{a5} &&+ v_c\,\bar{\epsilon}_{c5} \\
\epsilon_6 &= \bar{\epsilon}_{a6} &&= \bar{\epsilon}_{c6}.
\end{aligned} \tag{6}$$

Of Equations 5 and 6, all are exact except those giving ϵ_1, ϵ_2 and ϵ_6. The fractional error in each of those is of the same order as the ratio thickness/width of the layers. Since the layer thickness is at most only *c.* 300 Å but the width is of macroscopic sample size (of minimum dimension at least 0.05 cm), the complete set of Equations 5 and 6 are true to a high degree of accuracy for the present model.

Equations 3 and 4 apply at every point in phases A and C respectively and the phases are assumed homogeneous. These equations may, therefore, be rewritten in terms of volume average quantities

$$\bar{\epsilon}_a = \mathbf{S}_a\,\bar{\sigma}_a + \mathbf{e}_a\,(\triangle T) \tag{7}$$

$$\bar{\epsilon}_c = \mathbf{S}_c\,\bar{\sigma}_c + \mathbf{e}_c\,(\triangle T). \tag{8}$$

Equations 5 to 8 may then be readily solved for the terms of $\boldsymbol{\varepsilon}$ for arbitrary $\boldsymbol{\sigma}$ and $\triangle T$ to yield, from Equation 2, explicit expressions for $\mathbf{S}$ and $\mathbf{e}$ in terms of the phase properties $\mathbf{S}_a$, $\mathbf{S}_c$, $\mathbf{e}_a$ and $\mathbf{e}_c$ and phase volume fractions v_a and v_c. In the special case of $\alpha + \Omega = 0$ the terms of $\mathbf{S}$ are equal to those written out for model I of their paper by Maeda *et al* [8], apart from a few printing errors [Kawai – private communication].

3.3. Phase properties

In order to calculate $\mathbf{S}$ and $\mathbf{e}$, numerical values must first be assigned to all terms of $\mathbf{S}_a$, $\mathbf{S}_c$, $\mathbf{e}_a$ and $\mathbf{e}_c$.

Since phase A represents non-crystalline LPE it was assumed at this stage to be isotropic, with thermoelastic properties specified by a shear modulus G_a, Poisson's ratio ν_a and linear thermal expansivity e_a. Constituent terms of $\mathbf{S}_a$ and $\mathbf{e}_a$ were, therefore, assumed independent of Ω and given by

$$\begin{aligned}
S_{a11} = S_{a22} = S_{a33} &= \frac{1}{2G_a\,(1+\nu_a)} \\
S_{a12} = S_{a23} = S_{a13} &= \frac{-\nu_a}{2G_a\,(1+\nu_a)} \\
S_{a44} = S_{a55} = S_{a66} &= \frac{1}{G_a} \\
S_{a15} = S_{a25} = S_{a35} &= S_{a46} = 0 \\
e_{a1} = e_{a2} &= e_{a3} = e_a \\
e_{a5} &= 0.
\end{aligned} \tag{9}$$

For a given temperature T, G_a was equated to the real part of the complex shear modulus of amorphous LPE $G_a'^T$ (0.67 Hz), estimated by extrapolation by Gray and McCrum [19]. The Poisson's ratio ν_a is unknown: it was expected to lie between $\frac{1}{3}$ and $\frac{1}{2}$, from experience with other amorphous polymers [20]. The linear thermal expansivity, e_a was equated to that recently estimated by extrapolation by Buckley and McCrum [13].

The properties of phase C were derived with the aid of a subsidiary set of axes 1′, 2′, 3′ defined with 1′ parallel to *a*-axes, 2′ parallel to *b*-axes and 3′ parallel to *c*-axes (see Fig. 2). Numerical values of all elements of the compliance matrix $\mathbf{S}_c'$ and stiffness matrix $\mathbf{C}_c'$ (referred to axes 1′, 2′ 3′) of the orthorhombic polyethylene crystal are not yet known with certainty. Experimental and theoretical values for certain elements of the matrices were recently reviewed by Holliday and White [21]. The complete matrix $\mathbf{S}_c'$ or $\mathbf{C}_c'$ has so far been predicted, using differing models and numerical constants for the various inter and intramolecular interactions within the crystal, by Odajima and Maeda [22], Anand [23], Wobser and Blasenbrey [24] and Shiro and Miyazawa [25].

In the present work, the matrix $\mathbf{C}_c'$ calculated by Odajima and Maeda [22] was used (from Set I of their paper). Using, instead, the results of Wobser and Blasenbrey [24] would not have led to different conclusions, while the results of Anand [23] and Shiro and Miyazawa [25] were found to be incompatible* with the present experimental results and were not considered further.

Numerical values of the elements of $\mathbf{S}_c'$ were obtained by inverting the stiffness matrix $\mathbf{C}_c'$ given in Set I of their paper by Odajima and Maeda [22] for $T = -196°C$. They were as-

*Within the oriented sheets studied here *b*-axes had high preferential orientation parallel to *Y*. Since the sheets contained a more compliant non-crystalline fraction in addition to pure crystalline LPE we expect the condition $S_{c22}' < D_{90}$ to be satisfied. This was not the case for S_{c22}' as calculated by Anand and by Shiro and Miyazawa.

sumed constant over the temperature range from −196 to −80°C.

Thermal expansion of phase C with respect to axes 1′, 2′, 3′ was given by:

$$e_{c1}' = e_a, e_{c2}' = e_b, e_{c3}' = e_c, e_{c5}' = 0$$

where e_a, e_b and e_c are the linear thermal expansivities of the LPE crystal in a, b and c directions. For these quantities, the X-ray measurements of Davis *et al* [26] were used* (from the 2.5 h specimen of their paper).

The matrices $\mathbf{S}_c$ and $\mathbf{e}_c$ were obtained from $\mathbf{S}_c'$ and $\mathbf{e}_c'$ by reverting to the tensor form and rotating axes 1′, 2′, 3′ to coincide with 1, 2, 3, i.e. through an angle $(\alpha + \Omega)$ about axis 2′.

In assigning the above properties to the phases, two important assumptions have been implied:

1. both phases were assumed elastic, whereas at temperatures in the region of the γ-relaxation (*c.* − 130°C for a creep time t = 10 sec) phase A and possibly phase C show viscoelastic behaviour [19]. We, therefore, expect the equations to be exact in the relaxed and unrelaxed regions of temperature, but only approximations near the centre of the relaxation;

2. all strains were assumed infinitesimal, whereas for the range of temperatures considered, the values of e_a, e_a and e_b reach the order of 1% [13]. This difficulty could have been removed by choosing a reference temperature for e lower than 0°C. Conclusions drawn from the present work would not, however, have been significantly altered.

4. Comparison of model predictions with experimental results

4.1. Calculation of model predictions

To facilitate comparison of the computed **S** and **e** with experiment their reference axes 1, 2, 3 were rotated by $-\Omega$ about axis 2, to coincide with a further set of axes 1″, 2″, 3″ defined parallel to X, Y, Z (see Fig. 2). The resulting matrices $\mathbf{S}''$ and $\mathbf{e}''$ were computed for each oriented sheet (specified by its measured values of χ_v, α and Ω) over the range of temperature from − 196 to − 80°C.

As noted above, there existed no independent measurement of ν_a. Fortunately, however, the majority of terms in $\mathbf{S}''$ and $\mathbf{e}''$ were insensitive to ν_a, the term most critically dependent being S_{33}'' when $\alpha = \Omega = 0$. In the first instance, therefore, a constant value for ν_a of 0.460 was chosen, which gave the best overall fit between theoretical and experimental determinations of S_{33}'' for biaxially hot-drawn LPE. The resulting terms S_{pq}'' of $\mathbf{S}''$ are plotted as functions of temperature T in Figs. 3 and 4 for biaxially hot-drawn and biaxially cold-drawn LPE, respectively.

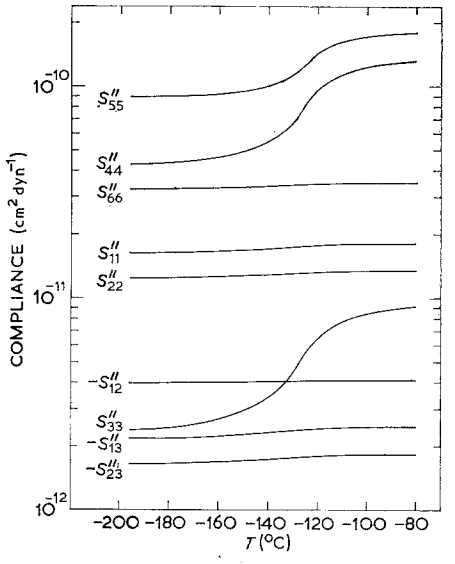

Figure 3 The terms of the compliance matrix $\mathbf{S}''$ predicted by the model for biaxially hot-drawn LPE plotted logarithmically versus temperature T.

Consider Fig. 3 for biaxially hot-drawn LPE. In this case, $\alpha = \Omega = 0$ and, therefore, $S_{15}'' = S_{25}'' = S_{35}'' = S_{46}'' = 0$. Of the remaining terms S_{pq}'', both their magnitudes and their relative increases at the γ-relaxation are predicted to be highly anisotropic. In particular, a large γ-relaxation is predicted in terms S_{33}'', S_{44}'' and S_{55}'' for which, from Equations 5 and 6, approximately series coupling exists between the phases.

Now consider Fig. 4a for biaxially cold-drawn LPE. The dominant effect of non-zero α and Ω is clearly the occurrence of relaxation in S_{11}'', S_{13}'' and S_{66}'' in addition to S_{33}'' and S_{44}'' while relaxation in S_{55}'' is partially suppressed. The extra terms S_{15}'', S_{25}'', S_{35}'' and S_{46}'' arising in this case are shown in Fig. 4b. For the complete model comprising mirror-image stacks they are all identically zero, equal and opposite contributions being made by the two halves of the model. They simply correspond to equal and opposite rotations of n_1 on application of an

*Strictly, this procedure ignores the effect of thermal stresses on the results of Davis *et al*: in practice the error involved is negligible.

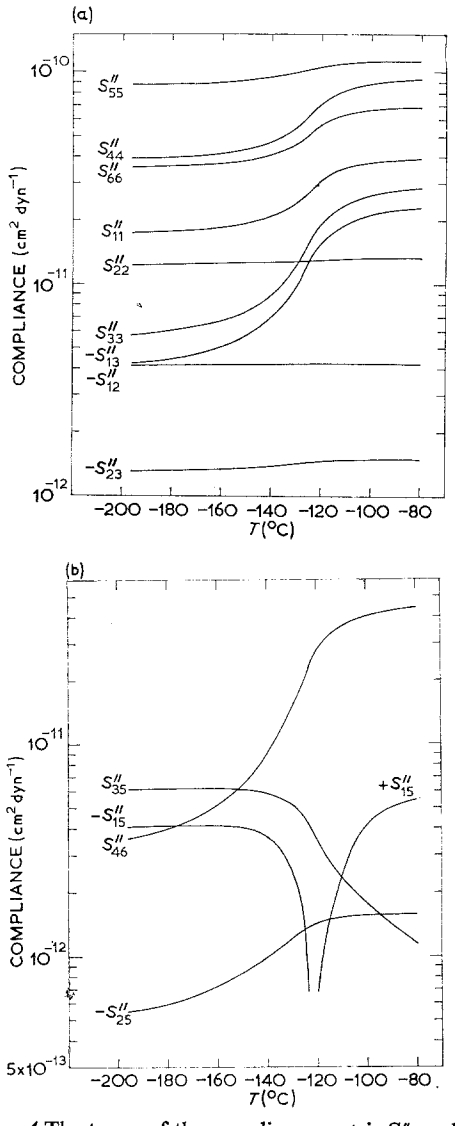

Figure 4 The terms of the compliance matrix S″ predicted by the model for biaxially cold-drawn LPE plotted logarithmically versus temperature T.

applied stress σ_1, σ_2 or σ_3 or shear stress σ_4 or σ_6. The occurrence of terms S_{25}'', S_{35}'' and S_{46}'' causes the model comprising two, bonded, mirror-image halves to be strictly* inapplicable in the presence of a shear stress σ_5 or σ_6.

4.2. Comparison with experiment

The present model predicts all seventeen terms of S″ and e″ in the general case of arbitrary α and Ω. Only the following however were available from experiment for comparison:

$$\begin{aligned} S_{33}'' &= D_0 \\ S_{22}'' &= D_{90} \\ S_{44}'' + 2S_{23}'' &= 4\,D_{45} - (D_0 + D_{90}) \\ e_1'' &= e_x \\ e_2'' &= e_y \\ e_3'' &= e_z. \end{aligned} \tag{10}$$

For those terms in which reasonable variations in ν_a caused a greater than 5% change, extreme possibilities $\nu_a = 0.333$ and $\nu_a = 0.500$ were evaluated in addition to $\nu_a = 0.460$, in order to indicate the dependence on ν_a. The terms of S″ are compared with experiment in Figs. 5 and 6, and the terms of e″ in Figs. 7 and 8, for biaxially hot-drawn and cold-drawn LPE respectively.

Comparing S_{33}'' in Figs. 5 and 6, the marked differences in compliance level [16] above the γ-relaxation observed in D_0 for the two types of oriented LPE are apparently explained by the model. Fig. 5 shows the dominant role played by ν_a in determining S_{33}'' when $\alpha = \Omega = 0$. Clearly, if ν_a were allowed to increase with increasing

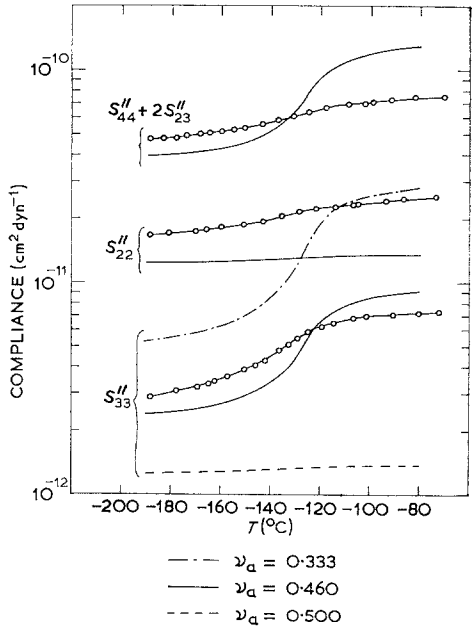

Figure 5 Comparison of model predictions with experimental compliance measurements (0) for biaxially hot-drawn LPE.

*The model may, however, be applied loosely in the presence of σ_5 or σ_6 by first allowing the twin stacks to be unbonded at their interface and, hence, able to deform independently, then taking for each term of ϵ the average of those for the two independent stacks.

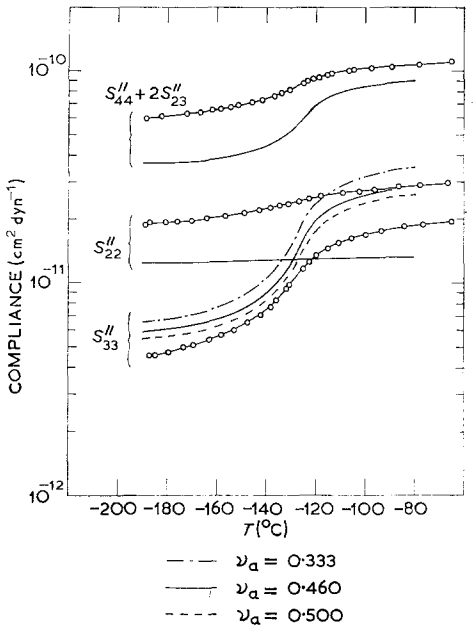

Figure 6 Comparison of model predictions with experimental compliance measurements (0) for biaxially cold-drawn LPE.

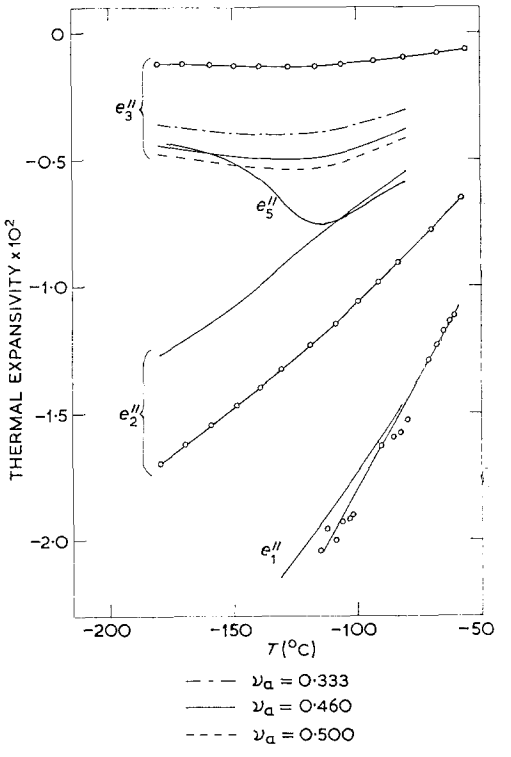

Figure 8 Comparison of model predictions with experimental thermal expansivity measurements (0) for biaxially cold-drawn LPE.

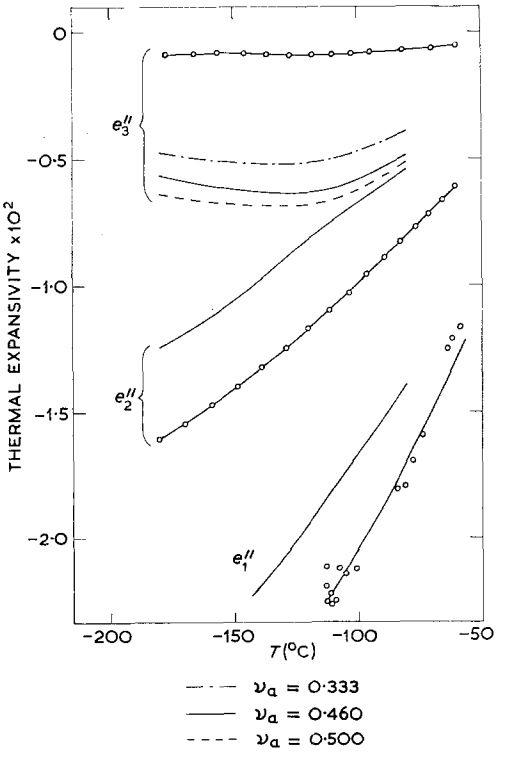

Figure 7 Comparison of model predictions with experimental thermal expansivity measurements (0) for biaxially hot-drawn LPE.

temperature an even closer fit between theory and experiment could be obtained for S_{33}''.

The comparisons between theory and experiment for S_{22}'' show the same pattern for both oriented sheets. In each case the small observed γ-relaxation is correctly predicted, although there are discrepancies in the precise compliance levels and relaxation magnitudes obtained from theory and experiment.

Comparing the calculated quantities (S_{44}'' + $2S_{23}''$) with experiment, their magnitudes are seen to be given approximately by the model. The observed γ-relaxation magnitude, however, is considerably smaller than that predicted, for both oriented sheets. Since the sum (S_{44}'' + $2S_{23}''$) is dominated by S_{44}'' (always contributing at least 96%), we conclude that the γ-relaxation in S_{44}'' is partially suppressed in the real oriented sheets.

When the calculated terms of $\mathbf{e}''$ are compared with experiment (Figs. 7 and 8) the result is similar to that obtained when applying simple series (for e_z) or parallel (for e_x and e_y) models [13]. Again the overall pattern of anisotropy is

correctly predicted but substantial discrepancies remain on the quantitative level. In the present case, however, these discrepancies carry greater significance, in view of the much closer correspondence between the present model and the polymer microstructure. In Fig. 8 is included the thermal shear e_5'' which arises for biaxially cold-drawn LPE. For the complete model it is identically zero, since the mirror-image halves make equal and opposite contributions. In this case, e_5'' simply corresponds to equal and opposite rotations of n_1 in the ZX plane when temperature is changed.

5. Discussion

The predictions of the model presented here are in qualitative accord with experiment, considering that the only adjustable parameter is ν_a to which most terms are insensitive. There are however, discrepancies on a quantitative level. How may these be explained? There are three most likely causes.

1. Some or all of the phase properties $\mathbf{S}_a$, $\mathbf{S}_c$, $\mathbf{e}_a$ and $\mathbf{e}_c$, and indirectly χ_v, may be in error.

2. The real oriented sheet contains a distribution of directions of n_1 and a-, b- and c-axes.

3. The model shown in Fig. 2 is not truly applicable since, although the real oriented sheet comprises similar stacks of alternating lamellar layers, the stacks are of much smaller dimensions in X and Y directions than portrayed in the model.

All of these possibilities certainly contribute in some degree to the discrepancies observed. The likely errors arising from items (1) and (2), however, cannot account for the most pronounced differences between model predictions and experiment. It appears that item (3) plays the dominant role.

Consider the effects of replacing the model of Fig. 2 by a more realistic model composed of many stacks of lamellae, identical to the stacks whose properties were previously calculated but of reduced dimensions in X and Y directions. A tendency towards narrower stacks has three effects. Firstly, the expressions for ϵ_1, ϵ_2 and ϵ_6 in Equations 6 become progressively less accurate because of "edge-effects". Secondly, these "edge-effects" within amorphous and crystalline layers begin to cause measurable non-linear material behaviour. This problem is well known in the context of materials reinforced by lamination [27-30]: it arises because of the severe shear stress concentration which occurs at the line junction between an edge and an interface in a composite laminated solid [27]. Thirdly, the precise mechanism of bonding and the nature of the interfacial region between adjacent stacks assume increasing importance.

The available evidence [1, 2, 6] suggests that, although a real drawn and annealed sheet of LPE comprises stacks of lamellae which are much narrower than those of Fig. 2, their widths remain at least several times the lamella thickness. The contribution of "edge-effects" is, therefore, unlikely to be dominant, but cannot be ruled out in the absence of more definite microstructural information. The most likely source of error lies in the interaction and nature of the interface between adjacent stacks. All the discrepancies between model predictions and experiment observed here could be readily explained by allowing (a) some mutual reinforcement (owing to mismatch between A and C layers) of bonded neighbouring stacks, and (b) the existence of some non-crystalline polymer interposed between groups of bonded stacks.

It may be significant that a simple model consisting only of uniform stacks of alternating crystalline and amorphous layers was also found by Goffin *et al* [31] to be inadequate for explaining anisotropy of the linear thermal expansivity of certain rolled and annealed sheets of branched polyethylene. These authors concluded that between the stacks of lamellae exists polymer without a regular lamellar texture. Their suggestion, similar to that of Maeda *et al* [32] for drawn and annealed LPE, was that after annealing there remains a remnant of the original as-rolled or as-drawn texture, giving a heterogeneous microstructure of which the stacks of lamellar layers form only one part. Such a situation, if it exists in the present oriented sheets, could explain some but not all of the results reported here.

6. Conclusions

The present work has shown how, if an oriented sheet of LPE is assumed to consist entirely of a two-phase composite laminate structure, it may be represented by a simple three-dimensional model. Straightforward thermoelastic analysis of the model yields predictions of the complete elastic and thermal expansion anisotropy of the sheet. Comparisons of model predictions with experimental results show extensive qualitative agreement. The composite laminate model, therefore, appears to provide, at least for drawn

and annealed LPE, a means of making exhaustive but qualitative predictions of elastic and thermoelastic behaviour. The model assumes a microstructure comprising only wide stacks of alternating lamellar layers of crystalline and non-crystalline polymer. Discrepancies observed between model predictions and experimental results suggest that the interfacial region between adjacent stacks also influences elastic and thermal expansion anisotropy.

Acknowledgements

The author thanks Dr N. G. McCrum for his advice and encouragement throughout the course of this work and Professor W. S. Hemp for several helpful discussions. The Science Research Council provided financial support.

References

1. K. SAKAOKU and A. PETERLIN, *J. Macromol. Sci. B* **1** (1967) 103.
2. A. PETERLIN and K. SAKAOKU, *J. Appl. Phys.* **38** (1967) 4152.
3. E. W. FISCHER and H. GODDAR, *J. Polymer Sci. C* **16** (1967) 4405.
4. E. W. FISCHER and G. F. SCHMIDT, *Angew. Chem.* **74** (1962) 551.
5. R. HOSEMANN, *J. Polymer Sci. C***20** (1967) 1.
6. J. LOBODA-CACKOVIC, R. HOSEMANN and W. WILKE, *Kolloid Z. u.Z. Polymere* **235** (1969) 1162.
7. P. H. GEIL, "Polymer Single Crystals" (Interscience, New York, 1963).
8. M. MAEDA, S. HIBI, F. ITOH, S. NOMURA, T. KAWAGUCHI and H. KAWAI, *J. Polymer Sci. A-2* **8** (1970) 1303.
9. J. C. HALPIN and J. L. KARDOS, *J. Appl. Phys.* **43** (1972) 2235.
10. A. J. OWEN and I. M. WARD, *J. Mater. Sci.* **6** (1971) 485.
11. C. P. BUCKLEY, R. W. GRAY and N. G. MCCRUM, *J. Polymer Sci. B* **7** (1969) 835.
12. *Idem, ibid* **8** (1970) 341.
13. C. P. BUCKLEY and N. G. MCCRUM, *J. Mater. Sci.* **8** (1973) 1123.
14. M. TAKAYANAGI, K. IMADA and T. KAJIYAMA, *J. Polymer Sci. C* **15** (1966) 263.
15. C. P. BUCKLEY, D.Phil. Thesis, Oxford University (1971).
16. C. P. BUCKLEY and N. G. MCCRUM, *J. Mater. Sci.* **8** (1973) 928.
17. J. A. SAUER, A. E. WOODWARD and N. FUSCHILLO, *J. Appl. Phys.* **30** (1959) 1488.
18. J. F. NYE, "Physical Properties of Crystals" (Oxford University Press, London, 1957).
19. R. W. GRAY and N. G. MCCRUM, *J. Polymer Sci. A-2* **7** (1969) 1329.
20. P. S. THEOCARIS and C. HADJIJOSEPH, *Kolloid Z. u.Z. Polymere* **202** (1965) 133.
21. L. HOLLIDAY and J. W. WHITE, *Pure and Applied Chemistry* **26** (1971) 545.
22. A. ODAJIMA and T. MAEDA, *J. Polymer Sci. C* **15** (1966) 55.
23. J. N. ANAND, *J. Macromol. Sci. B* **1** (1967) 445.
24. G. WOBSER and S. BLASENBREY, *Kolloid Z u.Z. Polymere* **241** (1970) 985.
25. Y. SHIRO and T. MIYAZAWA, *Bull. Chem. Soc. Japan* **44** (1971) 2371.
26. G. T. DAVIS, R. K. EBY and J. P. COLSON, *J. Appl. Phys.* **41** (1970) 4316.
27. D. B. BOGY, *J. Appl. Mech.* **35** (1968) 460.
28. M. S. HESS, *J. Comp. Mater.* **3** (1969) 630.
29. A. H. PUPPO and H. A. EVENSEN, *ibid* **4** (1970) 204.
30. R. B. PIPES and N. J. PAGANO, *ibid* **4** (1970) 538.
31. A. GOFFIN, M. DOSIERE, J. J. POINT and M. GILLIOT, *J. Polymer Sci. C* **38** (1972) 135.
32. M. MAEDA, K. MIYASAKA and K. ISHIKAWA, *J. Polymer Sci. A-2* **8** (1970) 1865.

Received 30 May and accepted 9 July 1973.